

A study of the plasticity in the vortex matter across the second magnetization peak in a YBCO crystal via measurements of minor hysteresis loops

D PAL^{1,*}, S RAMAKRISHNAN¹, A K GROVER¹, D DASGUPTA²
and BIMAL K SARMA²

¹Tata Institute of Fundamental Research, Homi Bhabha Road, Mumbai 400 005, India

²Department of Physics, University of Wisconsin, Milwaukee, WI-53201, USA

*Email: dilip@tifr.res.in

Abstract. Results of an investigation of the path dependence of the critical current density J_c due to the plastic deformation of the flux line lattice in a weakly pinned $\text{YBa}_2\text{Cu}_3\text{O}_{7-\delta}$ (YBCO) crystal for $H \parallel c$ are reported. The procedure of minor hysteresis loops has been used to explore the path dependence of J_c and the metastability effects. Contrary to the behavior observed in low T_c systems, in YBCO it is found that at low temperatures, the multivaluedness in $J_c(H)$ could persist beyond the notional peak field H_p , at which the anomalous variation in $J_c(H)$ reaches its maximum value.

Keywords. Flux pinning; critical currents; $\text{YBa}_2\text{Cu}_3\text{O}_{7-\delta}$

PACS Nos 74.60.Ge; 74.60.Jg; 74.72.Bk

1. Introduction

The discovery of high temperature superconductors provided impetus to explore the rich variety in the vortex phase diagram, and the samples of $\text{YBa}_2\text{Cu}_3\text{O}_{7-\delta}$ (YBCO) system are perhaps the most investigated among all type II superconductors for this task [1]. The (theoretical) prediction of the melting [2] of pristine (pinning free) vortex lattice stimulated the emergence of newer ideas with respect to the collective behavior of the vortices in the presence of quenched random disorder (pins)/thermal fluctuations. At low temperatures, tuning the balance between the underlying pinning and the elastic interaction between the vortices produces a crossover (or a transition) between the ordered and disordered regions. At high temperatures, the thermal fluctuations could complicate the situation further. The outcome of the competing forces leads to the characteristic features, like, the occurrence of an anomalous maximum in critical current density (J_c), which is referred to as the second magnetization peak (SMP) (i.e., the fish-tail effect) or the peak effect (PE) [3–6]. Ever since critical current measurements were looked at carefully in weakly pinned samples of a low T_c superconductor, it became known that the thermomagnetic history of the sample could affect its measured J_c value [7]. This history dependence in $J_c(H, T)$ was argued to be a consequence of the topological defects, such as, dislocations created in the flux line

lattice (FLL), which in turn correlate with the amount of point disorder in the sample [8]. It is asserted that the presence of these dislocations, which cause plastic deformation of the FLL, originate at the onset of the PE and the density of the dislocations reaches a maximum value at the extremum position of the PE [5,8]. The recent magneto-optical [9], transport [10] and magnetization [11] studies have confirmed the existence of metastable states and thereby elucidated the thermomagnetic history dependence in the energy landscape of the pinned vortices in a variety of low [12,13] and high T_c superconductors [14,15]. Kokkaliaris *et al* [16] and Zhukov *et al* [17] have added a new flavor to these studies by exploring the metastable states that get accessed via tracings of the minor hysteresis loops (MHL) and via relaxation studies (i.e., by magnetic field sweep rate dependent experiments), respectively. Their studies also led to the discovery of anomalous negative creep phenomenon [17] in the PE region.

Despite numerous reports related to the thermomagnetic history effects, newer manifestations of the metastability still surface up in the (H, T) region of the anomalous variation in J_c [18,19]. Thus, the parameters which control the extent of spatial order of FLL correlations remain to be completely unmasked.

Early transport data of Steingart *et al* [7] in a niobium crystal revealed the following inequality:

$$J_c^{\text{FC}}(H) > J_c^{\text{rev}}(H) > J_c^{\text{for}}(H) [\equiv J_c^{\text{ZFC}}(H)] \quad \text{for } H \leq H_p \quad (1)$$

where J_c^{ZFC} and J_c^{FC} are the critical current densities for the vortex states prepared in the usual zero field-cooled (ZFC) and the field-cooled (FC) manner. $J_c^{\text{rev}}(H)$ corresponds to J_c of the vortex state obtained by reducing the field from above H_{c2} to a given H in an isothermal scan. H_p is the field at which the anomalous variation in $J_c(H)$ reaches its maximum value and it is considered to represent the limiting value above which $J_c(H)$ does not display any thermomagnetic history dependence [7,8,10–13]. No exceptions have so far been reported as regards the above inequality in the context of conventional low T_c superconductors which display the PE phenomenon. The collective pinning description of Larkin–Ovchinnikov (LO) [20] for the weakly pinned vortex matter is often invoked to understand the observed behavior. In the LO prescription, the volume V_c of the Larkin domain (within which the vortices remain correlated and respond like an elastic medium) relates inversely to J_c as

$$J_c B = [n_p \langle f_p^2 \rangle / V_c]^{1/2} \quad (2)$$

where n_p and f_p represent the density of pins and the elementary pinning force, respectively. Both these parameters do not have thermomagnetic history dependence, while V_c could depend on the path followed by the field and the temperature. For instance, Steingart *et al* [7] had surmised that while cooling a sample from its normal state in a field, the vortices get nucleated in the superconducting state around the pinning sites such that the radial (R_c) and longitudinal (L_c) correlation lengths of FLL are small, and $V_c (=L_c V_c^2)$, presumably, is at its minimum value. The temperature variation of $J_c^{\text{FC}}(H)$, therefore, perhaps gets governed entirely by the temperature variation of $\langle f_p^2 \rangle$, which monotonically increases as T decreases. On the other hand, in the ZFC mode, as the field is ramped up in the forward direction, the bundle of vortices invade the superconductor at a high velocity [21]. The interaction effects between the vortices, combined with the high driving force, perhaps allow the vortices to explore the more ordered configuration (as compared to that in the FC state) in the presence of pinning centers, such that $V_c^{\text{ZFC}} > V_c^{\text{FC}}$. As H progressively increases, the

interaction effects predominate and the V_c continues to increase so long as $J_c^{\text{ZFC}}(H)$ monotonically decreases. Once $J_c^{\text{ZFC}}(H)$ enters the region of an anomalous increase, the onset of decrease in V_c sets in and it reaches its minimum value at H_p . The equivalence between J_c^{ZFC} and J_c^{FC} at $H = H_p$, therefore, stands rationalized. Above H_p , the decrease in $J_c(H)$ is considered to be governed solely by the collapse of the pinning force, while approaching the irreversibility line. When the applied field is decreased isothermally from above H_{c2} towards the zero value, initially the $J_c(H)$ is path independent until it reaches the peak value at $H = H_p$. As the field is reduced below H_p , the correlation volume V_c does not increase at the same rate at which it decreased while increasing the field towards H_p from lower fields in the ZFC mode. The observation, $J_c^{\text{rev}}(H) > J_c^{\text{for}}(H) (\equiv J_c^{\text{ZFC}}(H))$ for $H \leq H_p$, therefore, implies insufficient annealing of the amorphous configuration existing at the peak position of J_c , while reducing the field from above H_{c2} .

As stated in the beginning, the phenomenon of an anomalous increase in J_c is observed in weakly pinned samples of high T_c cuprate superconductors as well [3,4,9,14–18]. However, in cuprates, the field-cooled configurations of the vortex matter are found to be more ordered than those prepared in the ZFC manner [14,15,22]. The inequality statement of eq. (1) can, therefore, be no longer valid for such specimen.

A convenient way to explore the manifestation of the inequality statement of eq. (1) in samples of low T_c superconductors has been the study of characteristic features of the minor hysteresis loops (MHL) [11,16,23]. The existence of a linear relationship [24] between J_c and the magnetization hysteresis, $\delta M(H) = M(H^{\text{rev}}) - M(H^{\text{for}})$, facilitates such a study. Here, $M(H^{\text{rev}})$ and $M(H^{\text{for}})$ are the magnetization values at a field H on the reverse and forward legs of the (minor) hysteresis loop. We report in this paper the results obtained from tracings of the minor hysteresis curves in a very weakly pinned single crystal of YBCO for $H \parallel c$. As in the case of specimen of low T_c systems, three types of minor curves [11] have been looked at in YBCO. They are the $M-H$ curves initiated from (i) the FC magnetization values $M_{\text{FC}}(H)$, (ii) the ZFC magnetization values, i.e., $M(H_{\text{for}})$ and (iii) the magnetization values on the reverse leg of the envelope loop, i.e., $M(H^{\text{rev}})$. In contrast to the data in low T_c systems, where the FC minor curves (type-I) overshoot the envelope hysteresis loop [11], in YBCO such minor curves remain well inside the envelope loop. The minor curves initiated from the forward leg (type-II) in YBCO also remain well under the reverse leg of the envelope loop, however, those initiated from the reverse leg (type-III) are seen to overshoot the forward envelope loop, which is analogous to the behavior observed in the low T_c systems. Further, in YBCO, the temperatures at which the anomalous behavior of the $M-H$ loop extends over a large field interval, the path dependence in $J_c(H)$ persists well beyond the notional peak field H_p , at which the magnetization attains the maximum value.

2. Experimental

The YBCO crystal (dimensions $\sim 0.5 \times 0.5 \times 0.04 \text{ mm}^3$, $T_c(0) = 93.2 \text{ K}$ with $\Delta T_c = 0.8 \text{ K}$) used in the present work is the same in which a sharp PE had been observed at very low fields in the ac susceptibility measurements [14]. Most of the crystal is twin free, with a few widely spaced ($\sim 50 \mu\text{m}$) twin planes running all the way across. It, however, also has some strands of twin planes near two corners, with average inter-twin spacing $\sim 2 \mu\text{m}$. The occurrence of the PE at low fields and the re-entrant characteristic in the locus of peak

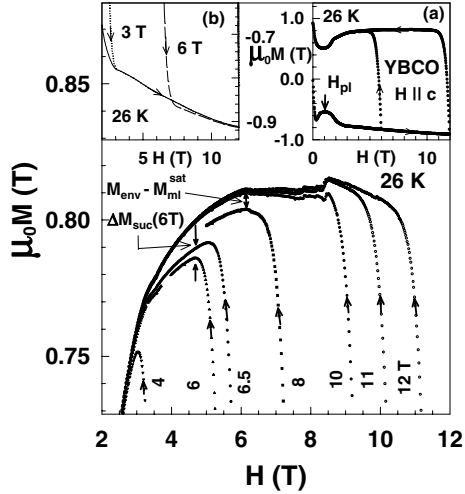


Figure 1. Isothermal $M-H$ loops and the minor curves (type-I) initiated from different field-cooled magnetization (M_{FC}) values. The inset panel (a) shows the envelope $M-H$ loop and the minor curves initiated from $M_{FC}(H)$ values at $H=3$ T and 9 T, respectively at 28.7 K. The main panel shows, on an expanded scale, the reverse leg of the envelope loop along with the portions of the FC minor curves initiated from different $M_{FC}(H)$ values. Note that the FC minor curves for $H < 10$ T undershoot the envelope loop over large field intervals, whereas the minor curve for $H = 10$ T (readily) merges into the envelope loop. The inset panel (b) shows, on an expanded scale, the reverse leg of the envelope loop along with portions of the two FC minor curves, one each for (i) $H < H_p$ and (ii) $H > H_p$, respectively at 62.6 K.

temperatures $T_p(H)$ just below $T_c(0)$ attests to the weak pinning nature of this crystal. Further, the same crystal also displays the presence of the second magnetization peak (SMP), which is distinct from the PE anomaly in the temperature interval 66–75 K. The magnetization hysteresis behavior in the present crystal is akin to the characteristic features reported earlier by others in their weakly pinned untwinned crystals of YBCO [25–27]. Below 72 K, the SMP and the PE anomalies move towards each other such that for 20 K $< T < 65$ K, the $M-H$ loops display a composite peak spreading over a large field interval. We have examined the three types of minor hysteresis loops as described above at different temperatures in the region of the composite anomalous variation. The important findings are depicted in figures 1 to 3. All the data have been recorded using a 12 T Vibrating Sample Magnetometer (Oxford Instruments, UK), with the magnetic field sweep rates ranging between 2 mT/s and 20 mT/s. While comparing the sets of minor curves at a given temperature, the same sweep rate is employed for all the curves.

3. Results

The two insets and the main panel of figure 1 show the $M-H$ loops (for $H \parallel c$) and the characteristic features of the FC minor curves (type-I) at 28.7 K and 62.6 K. The inset (a) gives an overview of the envelope loop and the minor curves initiated from $M_{FC}(H)$

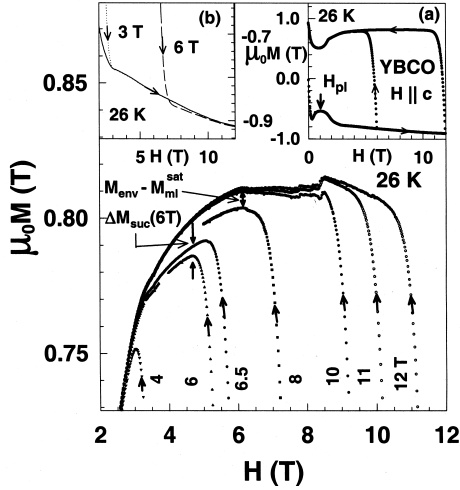


Figure 2. The inset panel (a) shows the envelope $M-H$ loop along with a minor curve (type-II) initiated from a field value (viz. 6 T) on the forward leg of the envelope loop. The main panel shows on an expanded scale the reverse leg of the envelope loop along with portions of the minor curves initiated from different fields (as indicated) on the forward leg of the envelope loop. The minor curves for $H \leq 10$ T undershoot the envelope loop, whereas that for $H = 11$ T readily merges into the envelope loop. $\Delta M_{\text{suc}}(6\text{ T})$ identifies the difference in saturated value of the magnetization of the 6 T minor loop and the magnetization value corresponding to the same field (i.e., the saturation field of 6 T minor loop) on the minor curve initiated from 6.5 T. $(M_{\text{env}} - M_{\text{ml}}^{\text{sat}})$, identifies the difference in the saturated value of the magnetization of 8 T minor loop and the magnetization value (at the saturated field of 8 T minor loop) on the reverse leg of the envelope loop. The inset panel (b) shows, on an expanded scale, portions of the two minor curves (type-III) initiated from fields of 3 T and 6 T, respectively, on the reverse leg of the envelope loop at 26 K. The continuous curve in panel (b) identifies the forward leg of the envelope loop. Note that the 6 T minor loop overshoots the (forward) envelope loop first, before merging into it.

values at $H = 3$ T and 9 T and progressed towards (i) the reverse and (ii) the forward directions, respectively. The FC minor curves in YBCO do not overshoot across the envelope curve. Such a response is unlike that reported in the samples of low T_c superconductors [11,13], where $J_c^{\text{FC}}(H) > J_c^{\text{rev}}(H)$. Instead, they appear to join the envelope loop, thereby, implying that $J_c^{\text{FC}}(H) \leq J_c^{\text{rev}}(H)$ in YBCO. The main panel of figure 1 focusses attention onto the detailed behavior as to how the minor curves initiated from different $M_{\text{FC}}(H)$ values merge into the reverse envelope loop at 28.7 K. Note first that the FC minor curve for $H = 10$ T merges into the (reverse) envelope loop within a field change of about 0.5 T. Such a behavior conforms to the canonical description of the critical state model, which assumes that $J_c(H)$ is a single valued function of H and predicts that a FC minor loop merges into the envelope loop as soon as the macroscopic currents start to flow inside the entire sample in response to a change in the external field [11]. The shape of the $M-H$ loop on reversal of field from 12 T indicates that the threshold field interval for reversing the sign of the macroscopic currents flowing throughout the sample is about 0.5 T. In this

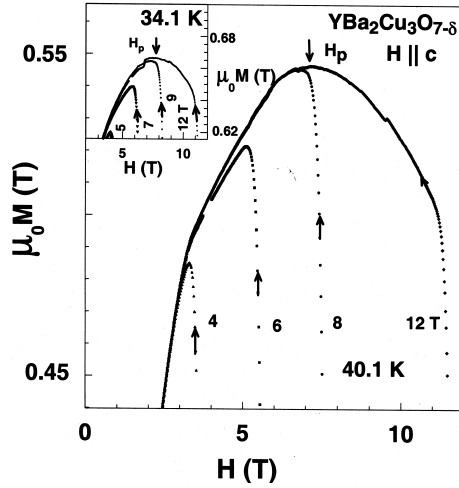


Figure 3. The main panel shows the minor hysteresis loops (type-II) initiated from different fields (as indicated) along with the reverse leg of the envelope loop at 40.1 K. Note that the minor loops for $H < H_p$ undershoot the envelope loop, whereas that for $H > H_p$ (cf. 8 T minor loop) readily merges into it. The inset panel shows the minor loops and envelope loops at 34.1 K. Note that at this temperature, the minor loop for 9 T ($> H_p$ at 34.1 K) undershoots the envelope loop.

context, note that the FC minor curve for 8 T does not merge into the envelope loop until the external field is reduced by about 2 T, i.e., it reaches the value 6 T. This could imply that the vortex configurations along the 8 T FC minor curve have J_c values lower than those of their counterparts along the reverse envelope curve. The feature of the existence of the differences between the reverse envelope loop and a FC minor curve over a substantial field interval can be noted for FC minor curves initiated from fields lying between 9 T and 3 T. The FC minor curve initiated from 2 T can be seen to readily merge into the reverse envelope curve once again, as it happens in the case of the minor curve initiated from 10 T. Thus, the metastability effects in $J_c(H)$ are evident in the field interval 3 to 9 T at 28.7 K. The anomalous behavior in $J_c(H)$ sets in at about 1 T at 28.7 K, however, cooling in a field $H > 1$ T does not freeze in the disorder corresponding to the maximum position of the anomalous variation in $M(H)$, as it happens in the case of samples of low T_c superconductors [11,13].

The inset (b) in figure 1 shows the FC minor curves initiated from 4 and 7 T, respectively at 62.6 K. At this temperature, the shape of the envelope $M-H$ loop is such that it displays a distinct maximum at about 5.5 T. Under this circumstance, the FC minor curves for $H > 5.5$ T readily merge into the reverse envelope curve, whereas those initiated from $H < 5$ T undershoot a little below the reverse envelope curve. This implies that $J_c^{FC}(H) \leq J_c^{rev}(H)$ for $H \leq H_p$ ($=5.5$ T) at 62.6 K.

The insets and the main panel of figure 2 show the characteristic features of the minor curves initiated from fields on the forward and reverse legs of the envelope curve at 26 K. Just as in figure 1, the inset (a) of figure 2 provides an overview of the minor curve initiated from 6 T in relation to the envelope $M-H$ loop (up to 12 T). Since the upper critical field at

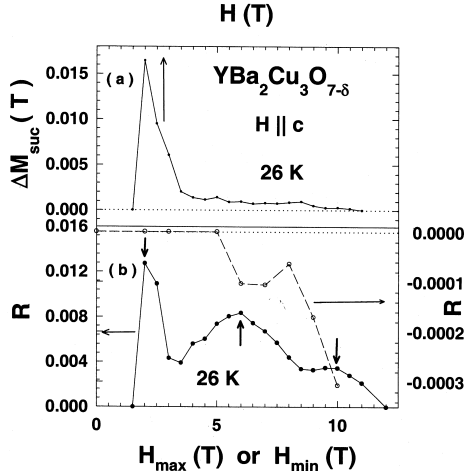


Figure 4. Panel (a) shows a plot of the differences in the successive minor loops (ΔM_{suc}) vs. field values from which the first of a given pair of successive minor loops (type-II) are generated at 26 K. Panel (b) shows plots of the parameter $R[(M_{\text{env}} - M_{\text{ml}}^{\text{sat}})/\Delta M_{\text{env}}]$ vs. field value (H_{max} or H_{min}) from which the minor loops of two types are initiated (type-II are filled circles; type-III are open circles).

26 K is far greater than 12 T, the so called envelope loop is essentially the minor hysteresis loop (MHL) obtained by reversal of field from 12 T on the forward leg. It is apparent that the other minor curves remain well within and merge into the 12 T MHL. The main panel of figure 2 shows, on an expanded scale, how the minor curves initiated from different fields on the forward leg merge into the envelope loop. The anomalous behavior in the M - H loop commences at about 1 T (cf. H_{pl} value in the inset (a) of figure 2), the minor curves initiated from $2 \text{ T} \leq H \leq 10 \text{ T}$ undershoot the (reverse) envelope loop. The 11 T minor loop, however appears to merge into the envelope loop in conformity with the prescription of the critical state model. The inset (b) of figure 2 shows how the minor curves initiated from 3 T and 6 T on the reverse leg merge into the (forward) envelope loop. It may be noted that while the 3 T minor loop readily merges into the envelope loop but the 6 T minor loop first overshoots the envelope loop, and later on merges into it after an interval of about 3 T. The feature of overshooting confirms that the vortex configurations on the reverse leg have higher J_c values than those on the forward leg.

The inset and the main panels of figure 3 show how the minor curves initiated from the forward leg merge into the (reverse) envelope at 34.1 K and 40.1 K, respectively. At both these temperatures, the peak position (H_p) of the anomalous variation in M - H can be well recognized. In the main panel at 40.1 K, note that while the minor curve initiated from 8 T ($> H_p$) readily merges into the envelope loop, the minor curves initiated from $H < H_p$ (e.g., 6 T and 4 T curves) undershoot the envelope loop. Such a response is analogous to the well-documented results in samples of low T_c superconductors, where $J_c^{\text{for}}(H) \leq J_c^{\text{rev}}(H)$ for $H < H_p$ [11,13]. However, the inset shows that at 34.1 K, the minor curve initiated from 9 T ($> H_p$ at 34.1 K) also undershoots the envelope curve, thereby implying that the metastability effects in $J_c(H)$ could persist beyond the peak position at this temperature.

4. Discussion

It is widely accepted [5,7,8] that the anomalous increase in $J_c(H, T)$ is associated with the commencement of plastic deformations in the well-ordered FLL due to proliferation of topological defects, like, dislocations as the pinning energy starts to dominate over elastic energy. Kokkaliaris *et al* [16] have recently prescribed procedures (i) to measure progressive change in the plasticity as the field is ramped up (or down) and (ii) to seek correlation between metastability in J_c and the path dependence (and the memory effects) in the extent of plasticity. The information on the metastability in J_c can be collated by comparing the saturated value of the magnetization of a given MHL with the magnetization value corresponding to the same field but lying on the neighboring (i.e., successive) minor loop. Following Kokkaliaris *et al* [16], we examined the differences ΔM_{suc} as a function of the initiating field H for pairs of MHL separated by 0.5 T. In figure 2, we identify one such difference, namely, ΔM_{suc} for $H = 6$ T. The non-zero value of this quantity implies an incremental change in plastic deformation of FLL between 6 and 6.5 T. We show a plot of ΔM_{suc} vs. H at 26 K in panel (a) of figure 4. ΔM_{suc} values appear to vanish above 10 T, thereby implying that the plastic deformation of the vortex solid reaches a saturation stage at a field $H_{\text{sat}} \approx 10$ T at 26 K. Kokkaliaris *et al* [16] had pointed out that $H_{\text{sat}} < H_p$ in their crystal of $\text{YBa}_2\text{Cu}_3\text{O}_{6.93}$ in the temperature range 68 K to 78 K, where the anomalous variation in $J_c(H)$ showed a distinct peak at H_p . Our data at 26 K, however, implies that when the anomalous variation in $J_c(H)$ is nearly independent of field and spread over a large field interval (2–10 T), the plastic deformation and path dependence in $J_c(H)$ extend up to a field value higher than the field limit at which the magnetization notionally reaches a maximum limit. As the temperature is raised to $T \geq 40$ K (cf. figure 3), $H_{\text{sat}} \leq H_p$ in our crystal as well. At this juncture, it is fruitful to recall that in a recent study on $\text{YBa}_2\text{Cu}_3\text{O}_{7-\delta}$ crystals with varying δ , Kokkaliaris *et al* [25] have reported that in a highly oxygenated crystal (with $\delta = 0.03$) having low density of oxygen vacancies, the path dependence in $J_c(H)$ at 66 K extends well above the peak field up to the highest field accessible in their experiment (i.e., 12 T). On the basis of their observations, they have sought [25] a correlation between the extent of quenched random disorder and the field range of plastic deformation [28,29] at a given temperature. However, in our crystal of YBCO, we find that for a given realization of quenched random disorder, the upper field limit of plastic deformation enhances as the temperature decreases.

To explore the memory effects in magnetization hysteresis, Kokkaliaris *et al* [16] have proposed the examination of the relative widths of the MHL and the envelope loop via the computation of the parameter R defined as $(M_{\text{env}} - M_{\text{ml}}^{\text{sat}}(H))/\Delta M_{\text{env}}$, where $M_{\text{ml}}^{\text{sat}}(H)$ is the saturated value of the magnetization of a MHL initiated from a given H , M_{env} is the magnetization obtained from the envelope loop but corresponding to the field value of the saturation magnetization of the MHL, and $\Delta M_{\text{env}} (\equiv M^{\text{rev}} - M^{\text{for}})$ represents the width of the envelope loop at the same field. As an example in figure 2, we have identified the difference $(M_{\text{ml}}^{\text{sat}}(H) - M_{\text{env}})$ for the MHL initiated from $H_{\text{max}} = 8$ T. In panel (b) of figure 4, we show the plots of the parameter R as a function of field (H_{max} or H_{min} for the MHL initiated from the forward (i.e., H_{max}) and the reverse legs (i.e., H_{min}), respectively on the envelope loop). Note first that the R values are positive and negative for the MHL of the type-II and the type-III, respectively, reflecting their undershooting and overshooting characteristics. The observation that they are not mirror image of each other alludes to the notion of the path dependence in the plastic deformation at a given H_{max} or H_{min} . The

oscillatory character of the R vs. H_{\max} curve further suggests the occurrence of a competition between the generation of topological defects, like, dislocations and their healing as H_{\max} increases at 26 K. The disordering effect of the quenched random inhomogeneities is known to enhance as the field increases, and the interaction between the vortices also strengthens as the inter-vortex spacing decreases in response to an increase in field. The shape of the R vs. H_{\max} at 26 K implies a rapid injection of dislocations near the onset position of anomalous variation in $J_c(H)$ at 2 T, followed by conspicuous additional injections near 4 T and 9 T, respectively. Thus, the process of the deformation of the elastic vortex solid at 26 K proceeds in a multi-step manner. At temperatures higher than 40 K, this multi-step process appears to reach its saturation limit at the peak field H_p , which in turn implies that the path dependence in $J_c(H)$ and the memory effects cease above the peak field at $T > 40$ K.

5. Summary

We have depicted new features via the study of minor hysteresis loops which explore the metastability effects in J_c and elucidate the path dependence in J_c due to plastic deformations induced in the vortex solid state of a YBCO crystal for $H\parallel c$ in the temperature region of the broad anomaly in J_c . The sample used in the study has some twin planes. However, it imbibes all the typical features [30] of magnetic hysteresis data in weakly pinned high quality untwinned single crystals of YBCO [25–27,30]. We note that at temperatures, where the fish-tail anomaly is broad, the process of plastic deformation happens in a multi-step manner and it continues up to a field value above which a rapid decline in the current density sets in. On increasing the field, while more of the plastic deformations are being caused, the process of the healing of the dislocations permeated earlier also goes on in response to the strengthening of the interaction effect. At temperatures, where the anomaly in J_c has a prominent maximum, all the manifestations of the path dependences in J_c and the plasticity effects cease at the field corresponding to the maximum in J_c . The feature that the field-cooled vortex solid in YBCO has $J_c(H)$ values smaller than those in the zero field-cooled state implies that the minor curves initiated from field-cooled magnetization values remain confined within the envelope hysteresis loop, this observation is in direct contrast to the behavior reported [11] in weakly pinned samples of low T_c superconductors, which display anomalous peak effect phenomenon. In the latter samples, the FC minor curves overshoot the envelope loop in a characteristic way before falling back onto the envelope loop. As yet, it is not completely obvious why the FC state in high T_c samples behaves differently from that in low T_c samples. The closer proximity of the peak field (H_p) to the irreversibility field (and H_{c2}) in low T_c samples [11,13,21] as compared to that in YBCO [14–16,27] could be one influencing factor. The other plausible reason could be the absence of the melting line and the irreversibility line in low T_c superconductors as compared to that of YBCO. In low T_c superconductors, the vortex state at the peak field H_p is termed as pinned amorphous [11–13], this amorphous state loses its pinning characteristics at the irreversibility field, which lies very close to the upper critical field where the vortices get nucleated. On the other hand, for the YBCO crystal the field-cooled state encounters the liquid state first, on further lowering the temperature the vortices enter into the pinned configurations on crossing the irreversibility line, which helps the FLL to arrange itself into a more symmetric (i.e., lower energy) state than that configured in the zero field-cooled state

at the same field compared to the field-cooled state. More investigations are clearly needed to completely understand the history dependence of the vortex configurations seen in the two classes of superconductors.

Acknowledgements

We would like to gratefully acknowledge many fruitful discussions with Shobo Bhattacharya, Mahesh Chandran, Heinz K pfer and Ashwin Tulapurkar. One of us (DP) would also like to acknowledge TIFR Endowment Fund for the award of Kanwal Rekhi Scholarship for Career Development.

References

- [1] G Blatter, M V Feigel'man, V B Geshkenbein, A I Larkin and V M Vinokur, *Rev. Mod. Phys.* **66**, 1125 (1994) and references therein
- [2] D R Nelson, *Phys. Rev. Lett.* **60**, 1973 (1988)
- [3] M Daeumling, J M Seuntjens and D C Larbalestier, *Nature (London)* **336**, 332 (1990)
- [4] B Khaykovich, E Zeldov, D Majer, T W Li, P H Kes and M Konczykowski, *Phys. Rev. Lett.* **76**, 2555 (1996)
- [5] M J Higgins and S Bhattacharya, *Physica C* **257**, 232 (1996) and references therein
- [6] P W Anderson, Basic Notions in Condensed Matter Physics, in *Frontiers in Physics* (Addison-Wesley Inc, USA, 1984) Vol. 55
- [7] M Steingart, A G Pute and E J Kramer, *J. Appl. Phys.* **44**, 5580 (1973)
- [8] R Wordenweber, P H Kes and C C Tsuei, *Phys. Rev.* **B33**, 3172 (1986)
- [9] C J van der Beek, S Colson, M V Indenbom and M Konczykowski, *Phys. Rev. Lett.* **84**, 4196 (2000)
- [10] W Henderson, E Y Andrei, M J Higgins and S Bhattacharya, *Phys. Rev. Lett.* **77**, 2077 (1996)
W Henderson, E Y Andrei and M J Higgins, *Phys. Rev. Lett.* **81**, 2352 (1998)
- [11] G Ravikumar, V C Sahni, P K Mishra, T V C Rao, S S Banerjee, A K Grover, S Ramakrishnan, S Bhattacharya, M J Higgins, E Yamamoto, Y Haga, M Hedo, Y Inada and Y Onuki, *Phys. Rev.* **B57**, R11069 (1998)
G Ravikumar, V C Sahni, P K Mishra, T V C Rao, S S Banerjee, A K Grover, S Ramakrishnan, P L Gammel, D J Bishop, E Bucher, M J Higgins and S Bhattacharya, *Phys. Rev.* **B61**, 12490 (2000)
- [12] S S Banerjee, N G Patil, S Saha, S Ramakrishnan, A K Grover, S Bhattacharya, G Ravikumar, P K Mishra, T V Chandrasekhar Rao, V C Sahni, M J Higgins, E Yamamoto, Y Haga, M Hedo, Y Inada and Y Onuki, *Phys. Rev.* **B58**, 995 (1998)
S S Banerjee, N G Patil, S Ramakrishnan, A K Grover, S Bhattacharya, G Ravikumar, P K Mishra, T V Chandrasekhar Rao, V C Sahni, M J Higgins, C V Tomy, G Balakrishnan and D Mck Paul, *Phys. Rev.* **B59**, 6043 (1999)
S S Banerjee, N G Patil, S Ramakrishnan, A K Grover, S Bhattacharya, G Ravikumar, P K Mishra, T V Chandrasekhar Rao, V C Sahni and M J Higgins, *Appl. Phys. Lett.* **74**, 126 (1999)
- [13] S Sarkar, D Pal, S S Banerjee, S Ramakrishnan, A K Grover, C V Tomy, G Ravikumar, P K Mishra, V C Sahni, G Balakrishnan, D Mck Paul and S Bhattacharya, *Phys. Rev.* **B61**, 12394 (2000)
- [14] D Pal, D Dasgupta, Bimal K Sharma, S Bhattacharya, S Ramakrishnan and A K Grover, *Phys. Rev.* **B62**, 6699 (2000)

- [15] S O Valenzuela and V Bekeris, *Phys. Rev. Lett.* **84**, 4200 (2000)
- [16] S Kokkaliaris, P A J de Groot, S N Gordeev, A A Zhukov, R Gagnon and L Taillefer, *Phys. Rev. Lett.* **82**, 5116 (1999)
- [17] A A Zhukov, S Kokkaliaris, P A J de Groot, M J Higgins, S Bhattacharya, R Gagnon and L Taillefer, *Phys. Rev.* **B61**, R886 (2000)
- [18] H K pfer, A Will, R Meier-Hirmer, Th Wolf and A A Zhukov, *Phys. Rev.* **B63**, 214521 (2001)
- [19] S O Valenzuela and V Bekeris, *Phys. Rev. Lett.* **86**, 504 (2001)
- [20] A I Larkin and Yu N Ovchinnikov, *Sov. Phys. JETP* **38**, 854 (1974)
A I Larkin and Yu N Ovchinnikov, *J. Low Temp. Phys.* **34**, 409 (1979)
- [21] S S Banerjee, S Saha, N G Patil, S Ramakrishnan, A K Grover, S Bhattacharya, G Ravikumar, P K Mishra, T V C Rao, V C Sahni, C V Tomy, G Balakrishnan, D Mck Paul and M J Higgins, *Physica C* **308**, 25 (1998)
- [22] D J Bishop, P L Gammel, D A Huse and C A Murray, *Science* **255**, 165 (1992) and references therein
- [23] S B Roy and P Chaddah, *J. Phys. Condens. Matter* **9**, L625 (1997)
- [24] W A Fietz and W W Webb, *Phys. Rev.* **178**, 657 (1969)
- [25] S Kokkaliaris, A A Zhukov, P A J de Groot, R Gagnon, L Taillefer and T Wolf, *Phys. Rev.* **B61**, 3655 (2000)
- [26] K Deligiannis, P A J de Groot, M Oussena, S Pinfeld, R H Langan, R Gagnon and L Taillefer, *Phys. Rev. Lett.* **79**, 2121 (1997)
- [27] T Nishizaki, T Naito and N Kobayashi, *Phys. Rev.* **B58**, 11169 (1998)
- [28] T Giamarchi and P Le Doussal, *Phys. Rev. Lett.* **72**, 1530 (1994); *Phys. Rev.* **B52**, 1242 (1995)
- [29] J Kierfield, T Natterman and T Hwa, *Phys. Rev.* **B55**, 626 (1997)
- [30] D Giller, A Shaulov, Y Yeshurun and J Giapintzakis, *Phys. Rev.* **B60**, 106 (1999)
- [31] D Pal, S Ramakrishnan, A K Grover, D Dasgupta and Bimal K Sharma, *Phys. Rev.* **B63**, 132505 (2001)
D Pal, S Ramakrishnan and A K Grover, *Phys. Rev.* **B65**, 096502 (2002)